

Provided for non-commercial research and education use.
Not for reproduction, distribution or commercial use.



This article appeared in a journal published by Elsevier. The attached copy is furnished to the author for internal non-commercial research and education use, including for instruction at the authors institution and sharing with colleagues.

Other uses, including reproduction and distribution, or selling or licensing copies, or posting to personal, institutional or third party websites are prohibited.

In most cases authors are permitted to post their version of the article (e.g. in Word or Tex form) to their personal website or institutional repository. Authors requiring further information regarding Elsevier's archiving and manuscript policies are encouraged to visit:

<http://www.elsevier.com/authorsrights>



Contents lists available at ScienceDirect

Journal of Alloys and Compounds

journal homepage: www.elsevier.com/locate/jalcom

Third harmonic generation process in Al doped ZnO thin films

M. Abd-Lefdil^a, A. Douayar^a, A. Belayachi^a, A.H. Reshak^{b,c,*}, A.O. Fedorchuk^d, S. Pramodini^e, P. Poornesh^e, K.K. Nagaraja^f, H.S. Nagaraja^f^a Materials Physics Laboratory, University of Mohammed V-Agdal, P.B. 1014 Rabat, Morocco^b Institute of Complex Systems, FFPW, CENAKVA, University of South Bohemia in CB, Nove Hradky 37333, Czech Republic^c Center of Excellence Geopolymer and Green Technology, School of Material Engineering, University Malaysia Perlis, 01007 Kangar, Perlis, Malaysia^d Lviv National University of Veterinary Medicine and Biotechnologies, Department of Inorganic and Organic Chemistry, Lviv, Ukraine^e Nonlinear Optics Research Laboratory, Department of Physics, Manipal Institute of Technology, Manipal University, Manipal 576 104, Karnataka, India^f Materials Research Laboratory, Department of Physics, National Institute of Technology Karnataka, Surathkal, DK 575 025, Karnataka, India

ARTICLE INFO

Article history:

Received 20 July 2013

Received in revised form 21 August 2013

Accepted 22 August 2013

Available online 4 September 2013

Keywords:

Al doped ZnO thin films

Laser frequency generation

Photoinduced optical devices and electronics

Nonlinear optical studies

Optical limiting

ABSTRACT

We have performed studies on the third-order nonlinear optical susceptibility of Al doped ZnO (AZO) thin films using z-scan and third harmonic generation techniques. From the present studies, it reveals that the introduction of Al in ZnO leads to substantial changes in the third-order nonlinear susceptibility. Additionally we have shown that using treatment by the 707 nm laser pulses of the Er:glass 20 ns laser also influence on the third harmonic generation. Such behavior is explained by the photoinduced charge re-occupation of the trapping levels on the borders substrate and ZnO. Further, the sign and magnitude of nonlinear absorption coefficient β_{eff} , nonlinear refractive index n_2 , real and imaginary parts of third-order nonlinear susceptibility were evaluated. Finally, the optical limiting studies for various concentrations of AZO thin films were determined. Reverse saturable absorption was the dominant process leading to the observed nonlinear behavior.

© 2013 Elsevier B.V. All rights reserved.

1. Introduction

There are many works devoted to studies of the nonlinear optical properties of ZnO films [1,2]. Particular role belongs to the orientation of ZnO films with respect to the substrate [3] and the interface between the substrate and ZnO [4,5]. Most of the efforts were devoted to the formation of the refined technologies in order to improve the sample's quality, however Kityk et al. [6] established that even the use of simple spray deposition technology may be of interest for the nonlinear optical properties in the case when it is used the external photoinduced beam. For this reason, in one of the part in the present work, we will study a possibility of enhancement of the third harmonic generation for the Al doped ZnO films using treatment by the pulsed laser beam.

Following the results of studies of binary Al_2O_3 -ZnO system [7] the solubility of Al_2O_3 in ZnO at temperature below 1200 °C do not exceed 1% and during the enhancement of temperature the solubility of Al_2O_3 is partially enhanced. At higher content of Al_2O_3 there occurs a compound ZnAl_2O_4 with spinal structure which is in

equilibrium with Al_2O_3 . Exploring the compound structure within the phase existence of the solid solutions $(\text{Zn,Al})_{1-y}\text{O}$ and $(\text{Zn,Fe})_{1-x}\text{O}$ for $\text{Zn}_{0.943}\text{Al}_{0.038}\text{O}$ [8] at 1973 K it was shown that Al ions occupy the positions of Zn atoms.

An analysis of the crystalline structure for the binary compound system Al_2O_3 -ZnO system (Fig. 1) has shown for the two limiting cases of ZnO or $\text{Zn}_{0.943}\text{Al}_{0.038}\text{O}$ (Fig. 1a) (in Fig. 1a we have $\text{Zn}_{0.93}\text{Al}_{0.038}\text{O}$) as well as Al_2O_3 (Fig. 1c) [8] that the second coordination surrounding [9] for oxygen atoms is of the one type – in the form of hexagonal cubooctahedra. Within the one-type anion sub-system the metallic atoms are situated in the different voids. The Al atoms are situated opposite the fourth-angle planes in the octahedral and the Zn atoms are situated opposite the triangle planes in the tetrahedral voids. For the intermediate compound ZnAl_2O_4 (Fig. 1b) [10], which possesses the second coordination sphere in a form of cubooctahedra the metallic components occupy the same voids as well as in the starting binary compounds.

So the incorporation of Al into the structure of ZnO may lead to a slight solvation of Al atoms and may lead to varying anionic sub-lattice up to formation of ternary phase ZnAl_2O_4 . For the solid solution $\text{Zn}_{1-x}\text{Al}_x\text{O}$ the three-valence Al^{+3} ions substituting the two-valence atoms of Zn^{+2} in the range of existence of solid solution occupying non-proper for them tetrahedral coordinated bonds which form optical active centers. Outside the range of the solid

* Corresponding author at: Institute of Complex Systems, FFPW, CENAKVA, University of South Bohemia in CB, Nove Hradky 37333, Czech Republic. Tel.: +420 777 729 583; fax: +420 386 361 219.

E-mail address: maalidph@yahoo.co.uk (A.H. Reshak).

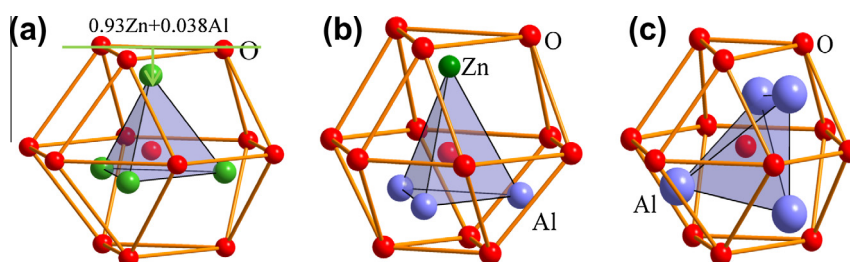


Fig. 1. Second coordination surrounding of the oxygen atoms and coordination surrounding for the compounds $Zn_{0.943}Al_{0.038}O$ (a), $ZnAl_2O_4$ (b) and Al_2O_3 (c).

state alloys existence the exceeded Al atoms are connected to form of the intermediate phase $ZnAl_2O_4$ possessing anionic sub-lattice of other types and which forms their grains and is not scattered on the borders of the output phase. This factor may play a decisive role for use of the photoinduced treatment.

We will explore the dependence of the THG versus the power density of the photo inducing laser beam as well as versus the doping content. Further, the sign and magnitude of real and imaginary parts of third-order nonlinear susceptibility was determined by using z-scan technique. Optical limiting, one of the application of nonlinear optics, was also carried out for different concentrations of AZO films. Section 2 describes technology of the sample's preparation and the z-scan experimental technique. Section 3 contains principal results of the structural and photoinduced THG measurements, the nonlinear absorption-refraction studies and the optical limiting behavior for AZO thin films together with the appropriate discussion.

2. Experimental

2.1. Sample preparation

Aluminum doped ZnO (AZO) thin films were deposited on glass substrate by spray pyrolysis technique. An homogeneous solution was prepared by dissolving zinc chloride ($ZnCl_2$) [0.1 M] and aluminum nitrate ($Al(NO_3)_3$) in distilled water at room temperature. Different solutions were prepared with different Al content. Some drops of acetic acid (CH_3COOH) have been added while stirring at room temperature for 30 min to obtain a clear solution. The glass substrate was cleaned in ethanol, rinsed in distilled water, and subsequently dried under nitrogen gas plate and heated progressively until the deposited temperature is reached. All films were deposited at $350^\circ C$ during 77 min with a flow rate of the solution fixed at 2.6 ml/min.

2.2. z-Scan experimental technique

The third-order nonlinear susceptibility $\chi^{(3)}$ of AZO thin films were evaluated by employing z-scan technique. z-Scan developed by Sheik-Bahae et al. [11,12] is a single-beam technique which offers simplicity as well as high sensitivity for measuring both nonlinear absorption (NLA) and nonlinear refraction (NLR) simultaneously. The schematic experimental setup used for z-scan technique is shown in Fig. 2. In the present experiment, a polarized Gaussian laser beam is tightly focused to a narrow waist using a lens. The sample is mounted on the micrometer translation stage and by translating the sample between $+z$ and $-z$ positions along the z -direction, the transmitted intensity through the sample is measured, with and without ($S=1$) the presence of aperture at far field in front of the photodetector. As the sample moves through the beam focus ($z=0$), self-focusing or self-defocusing modifies the wave front phase, there by modifying the detected beam intensity. Z-scan experiments were performed by using Thor labs HRP350-EC-1 CW He-Ne laser at 633 nm wavelength as an excitation source. The laser beam was focused

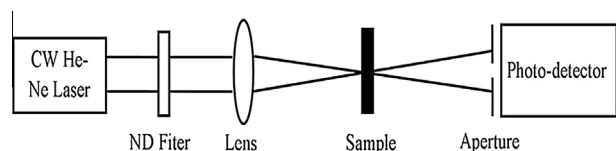


Fig. 2. Schematic z-scan experimental setup.

to a spot size of $36.78 \mu m$ and the Rayleigh length Z_R of 6.71 mm using a 5 cm focal length lens with input power 23 mW. The film thickness is less than the Rayleigh length Z_R and thus the thin sample approximation is valid [11,12].

Optical power limiting measurements were performed for the concentrations 1%, 3% and 5% of AZO thin films. The films were placed at the focal plane of the lens. The input power of the laser beam was varied by using neutral density filter and the resultant output power through the samples was recorded using a photodetector fed to Thor labs PM320E dual channel optical power and energy meter.

2.3. X-ray diffraction and surface morphology

X'Pert Pro diffractometer was used to determine the X-ray Diffraction (XRD) patterns with $Cu K\alpha_1$ radiation ($\lambda = 1.54056 \text{ \AA}$). Surface morphology of AZO thin films was performed by Atomic Force Microscopy (AFM, Dimension 3100).

3. Results and discussion

3.1. Structural and morphology

Fig. 3 shows the X-ray diffraction patterns of AZO thin films with different Al concentration. Both undoped and doped films have presented a polycrystalline single phase and all peaks correspond to ZnO wurtzite structure with a preferential orientation along the [002] direction. The lattice parameters, a and c , seem constant about 0.318 nm and 0.520 nm, respectively. From the XRD results we have determined the texture coefficient (TC), which represents the texture of particular plane, whose deviation from unity implies the preferred growth. The texture factor of particular plan is defined by relation [13]:

$$TC(hkl) = \frac{I(hkl)/I_0(hkl)}{n^{-1} \sum_n I(hkl)/I_0(hkl)}, \quad (1)$$

where $I(hkl)$ is the measured relative intensity of a plane (hkl), $I_0(hkl)$ is the standard intensity of the plane (hkl) taken from JCPDS data [89-1397], n the number of diffraction peaks. The results are summarized in Table 1. One can note that all the films present a preferential orientation along the [002] direction and the higher

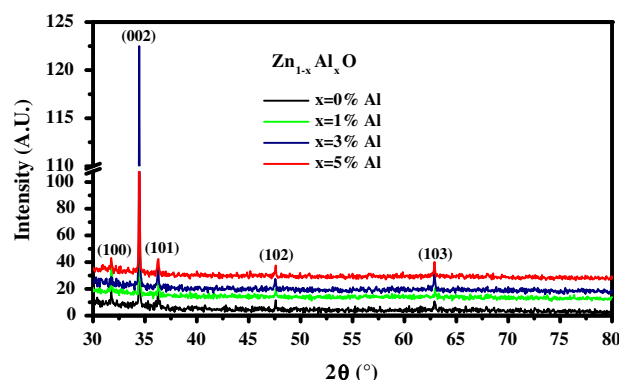


Fig. 3. XRD patterns of AZO sprayed thin films.

Table 1

Various structural parameters of AZO sprayed thin films. *x*: Al doping, *d*: thickness, *D*: crystallite size, TC: texture coefficient, δ : dislocation density, *N*: number of crystallites per unit surface area, ϵ : strain.

<i>x</i> (at.%)	<i>d</i> (nm)	<i>D</i> (nm)	TC (002)	δ (10^4 lines m^{-2})	<i>N</i> ($10^{14} m^{-2}$)	ϵ (10^{-4})
0	410	67	2.30	2.2	14	5.4
1	250	57	2.26	3.0	13	4.6
3	455	94	3.01	1.1	5.4	4.6
5	455	73	2.72	1.9	12	5.0

TC value for (002) plane was observed for thin film doped with 3% of Al. The increase in preferred orientation along (002) plane is associated to the increase in the number of grains along that plane. The average crystallites size of AZO thin films was estimated using the Scherrer's formula along the *c*-axis [14]:

$$D = \frac{0.9\lambda}{B \cos \theta} \quad (2)$$

where θ is the Bragg's diffraction angle of (002) plane, *B* is the broadening of diffraction line at half its maximum intensity and λ the wavelength of X-rays. *D* values, which give the coherence length perpendicularly to the substrate, are also listed in Table 1. We can note that the higher value was obtained for 3% Al content in agreement with the above TC values. This indicates that 3% of Al corresponds to the optimal value. Above this value, defects can be created, which can decrease both the texture and the grains size.

To support the last hypothesis, we have tried to extract some information's on the evolution upon doping of dislocations in our films. Using the size of crystallites *D* and the thickness *d*, the dislocation density δ , the number of crystallites *N* per unit volume and the strain ϵ are calculated using the following formula [15] and reported in Table 1:

$$\delta = \frac{1}{D^2}, \quad (3)$$

$$N = \frac{d}{D^3}, \quad (4)$$

$$\epsilon = \frac{\Delta(2\theta) \cos \theta}{4} \quad (5)$$

In accordance with the TC variation and *d* values, the small values of the strain and the dislocation density were observed for ZnO doped with 3% of Al. Hence, this sample presents the best crystalline quality.

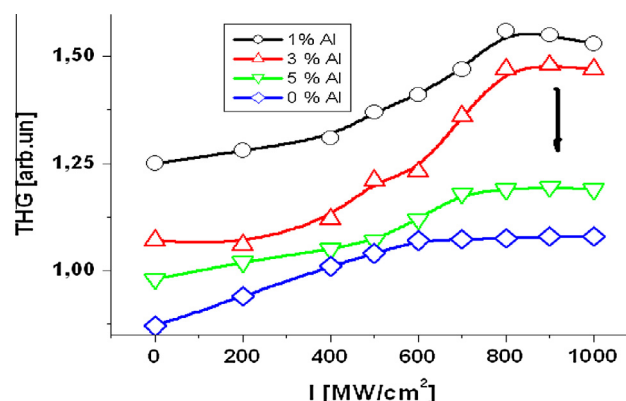


Fig. 5. Dependence of the THG versus the pumping power density.

Fig. 4 shows the AFM images of undoped and ZnO doped with 3% of Al deposited on glass substrates. From the surface morphology images, it can be seen that the in-plane grain size does not change much and only a small part of the grains increased. The surface roughness of the films depends on the aluminum doping content. We observed that AZO with 3% of Al showed a uniform grain size with the lowest root mean square (rms) value of about 24 nm, less than rms for undoped ZnO which was around 38 nm.

3.2. THG data

The dependence of the THG versus the pumping power densities are presented in Fig. 5. One can see that with increasing power density the output THG signal was substantially enhanced. This signal has achieved its maximum at about 600–800 MW/cm^2 . With further enhancement of the power densities for all the samples there occurred some saturation and even decrease of the THG.

The occurrence of such enhancement may be a consequence of a competition between the photoexcited and relaxation processes on the localized trapping levels. The THG dependences versus the Al Content have shown substantially non-monotonous dependences. And maximal increase was observed at 1% of Al. The further increase of the Al content leads to a suppression of the THG maximum.

Such behavior may be explained within a framework of multiphoton excitations which for the more Al content becomes preferable with respect to the third harmonic processes. Additionally some role begins to play the interface trapping levels.

Additional control of the photoinduced surfaces has shown that during the photoinducing processes the increase of temperature

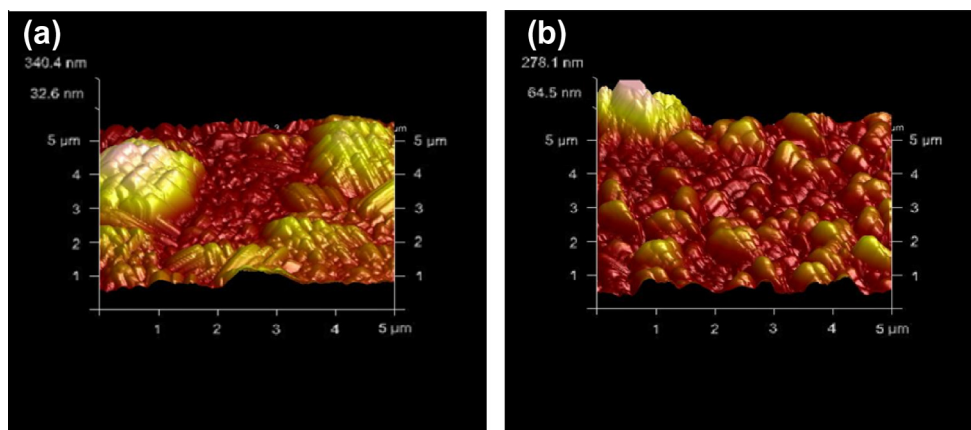


Fig. 4. AFM images of the surface of AZO sprayed thin films. (a) ZnO:0% Al, (b) ZnO:3% Al.

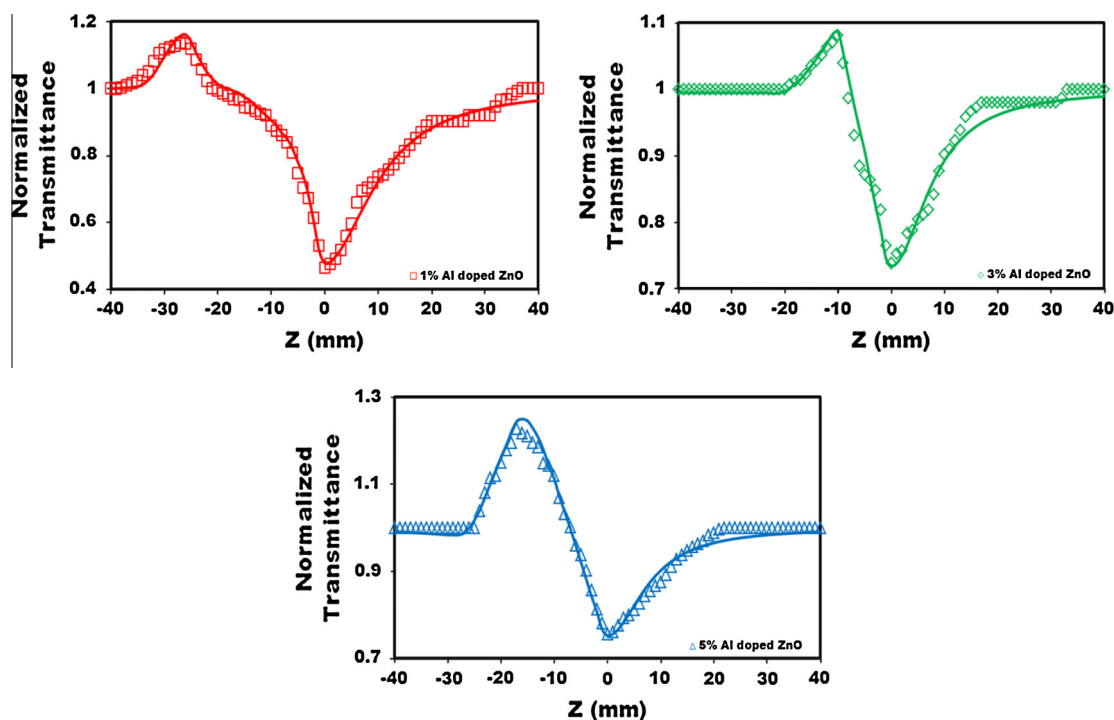


Fig. 6. Open aperture z-scan traces of 1%, 3% and 5% Al doped ZnO thin films.

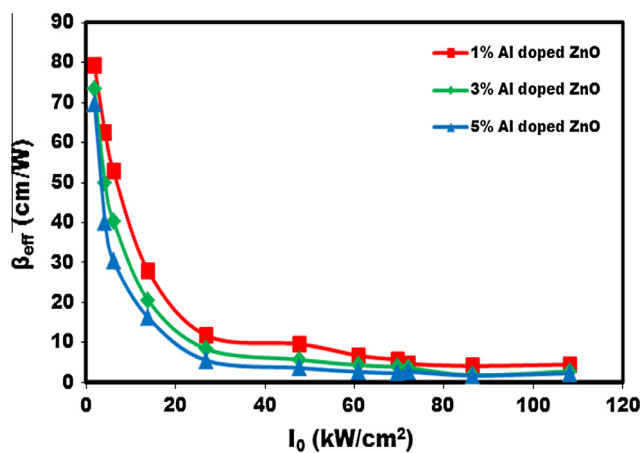


Fig. 7. Nonlinear absorption coefficient β_{eff} vs. on-axis input intensity I_0 of 1%, 3% and 5% Al doped ZnO thin films.

did not exceed 3–4 K. There were also not any signs of photodestructions. The results were averaged over more than 400 points on the sample's surface. The photoinduced THG signal was completely reversible and was absent after several ms. The THG signal was observed only during the overlap of the photoinducing and the fundamental beams.

3.3. Nonlinear optical studies using z-scan technique

Open aperture and closed aperture z-scan experiments were carried out in order to estimate the intensity dependence of nonlinear absorption and nonlinear refraction process for Al doped ZnO thin films at an input intensity of $1.08 \times 10^7 \text{ W/m}^2$. The open aperture z-scan measurements for Al doped ZnO thin films are shown in Fig. 6. When the samples are away from the focus, the light intensity is low. As it is seen clearly in the figure, as the film

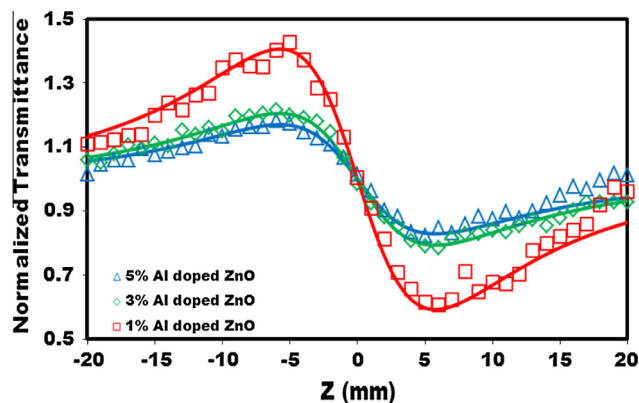


Fig. 8. Pure nonlinear refraction z-scan traces of 1%, 3% and 5% Al doped ZnO thin films.

is translated towards focus, the transmittance increases and depicts saturable absorption (SA) behavior. But as the sample approaches focus, the transmittance decreases and forms a valley indicating reverse saturable absorption (RSA) behavior. Variety of organic and inorganic samples reported in literature behaved the switch over behavior from SA to RSA and vice versa [16–21].

RSA behavior may results due to any of the nonlinear mechanisms such as two-photon absorption (TPA), excited state absorption (ESA), free carrier absorption (FCA), nonlinear scattering or with the combination of these processes [22]. The origin of RSA is based on the two conditions, (i) the molecules present in ground state and excited states can absorb the incident photons of same wavelengths and (ii) the absorption of excited states must be larger than that of the ground states. If the nonlinearity is due to two-photon absorption (TPA) alone, the nonlinear absorption coefficient β_{eff} should be a constant independent of on-axis input intensity I_0 [23]. But from Fig. 7, the nonlinear absorption coefficient β_{eff} values decreases with increase in on-axis input intensity I_0 which

Table 2
Third-order nonlinear optical parameters, optical limiting and clamping of AZO thin films.

Sample	β_{eff} (cm/W)	n_2 (esu)	$\chi_R^{(3)}$ (esu) $\times 10^{-3}$	$\chi_I^{(3)}$ (esu) $\times 10^{-3}$	Optical limiting (mW)	Optical clamping (mW)
1% Al doped ZnO	48.59	0.42	9.04	2.56	~7	~7.2
3% Al doped ZnO	23.81	0.22	4.82	1.25	~8.2	~8.8
5% Al doped ZnO	22.23	0.18	4.00	1.17	~9	–

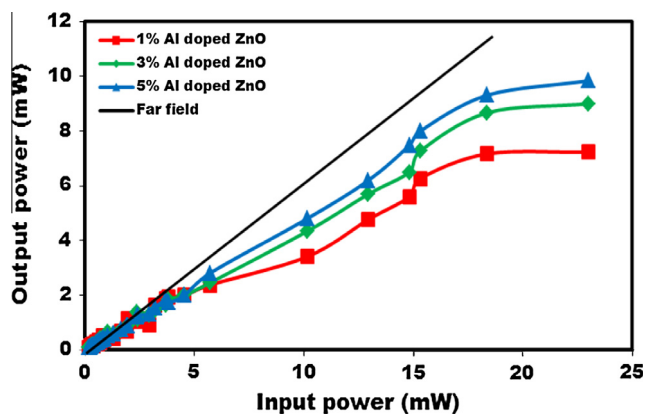


Fig. 9. Optical power limiting response of 1%, 3% and 5% Al doped ZnO thin films.

is the consequence of sequential two-photon absorption [23]. Compared to TPA, FCA is a weak process and hence its contribution to the nonlinear absorption is relatively less [24]. This suggests that a higher-order effect, such as FCA accessed via two-photon absorption is contributing to the NLA [24].

The closed aperture z-scan experiments were performed by placing the aperture in front of the detector, allowed us to determine the sign and magnitude of the nonlinear refractive index n_2 of Al doped ZnO thin films. Since closed aperture data obtained from z-scan will contain both nonlinear refraction and nonlinear absorption components, it is necessary to separate the nonlinear absorption components from the nonlinear refraction so as to extract pure nonlinear refraction. Fig. 8 illustrates the closed aperture z-scan profiles of the samples. The normalized closed aperture z-scan curve exhibits a pre-focal transmittance maximum (peak) followed by a post-focal transmittance minimum (valley) signature for the samples. This peak-valley signature indicates the self-defocusing property and it is represented by negative nonlinear refractive index n_2 . The sign of the nonlinear index of refraction n_2 of a sample is thus immediately clear from the shape of graph. The physical origin of nonlinear refraction can be electronic, molecular, electrostrictive or thermal in nature. The closed aperture z-scan curves for both samples show a peak-valley separation of $\sim 2 Z_R$. A peak-valley separation of more than 1.7 times the Rayleigh range (Z_R) is the clear indication of thermal nonlinearity. The nonlinear absorption and nonlinear refraction coefficients are determined from the open aperture and closed aperture z-scan data. The real and imaginary parts of the third-order nonlinear optical susceptibility $\chi^{(3)}$ is determined by using the nonlinear refractive index n_2 and nonlinear absorption coefficient β_{eff} by the following equations [23,24],

$$\chi_R^{(3)}(\text{esu}) = 10^{-4} \frac{\epsilon_0 c^2 n_2^2}{\pi} n_2 \text{ (cm}^2/\text{W)}, \quad (6)$$

and

$$\chi_I^{(3)}(\text{esu}) = 10^{-2} \frac{\epsilon_0 c^2 n_2^2 \lambda}{4\pi^2} \beta_{\text{eff}} \text{ (cm}^2/\text{W)}, \quad (7)$$

where ϵ_0 is the vacuum permittivity and c is the light velocity in vacuum. The obtained values of nonlinear refractive index n_2 ,

nonlinear absorption coefficient β_{eff} and the real and imaginary parts of the third-order nonlinear susceptibility of AZO thin films are given in Table 2.

3.4. Optical power limiting studies

Optical power limiters have received significant attention in order to control the intensity of light that are in demand for the development of optical technology. An ideal optical limiter is transparent to the incident laser light below a threshold level and above the threshold clamping of light takes place, thus providing complete safety to the optical sensors and human eyes. The optical limiting behavior for concentrations 1%, 3% and 5% of AZO thin films was studied without aperture ($s = 1$) under cw He–Ne laser illumination. Optical limiting measurements were carried out by placing the sample near the focal plane of the lens and the transmitted power through the sample is recorded for different input powers. Fig. 9 shows the characteristic optical limiting curves as a function of incident power varying from 0.2 up to 23 mW. The deviation from linearity is observed for all the films and it is tabulated in Table 2. The optical limiting threshold and optical clamping values for 1%, 3% and 5% of AZO thin films are given in Table 2. From Fig. 9 it is clear that for 1% AZO film, the optical clamping takes place. Whereas for the 3% and 5% AZO films, there is no clamping taking place. In the present case RSA is the leading process for the observed nonlinear absorption.

The results of the article are in a good agreement about the third-order susceptibilities performed in Ref. [25]. They have shown that the doping of the ZnO films favors a higher conductivity, and there is a big conversion of the third harmonic signal at different dopants and at an appropriate concentration. As in our case it was confirmed that the morphology and the crystalline quality of the films are the main factors for this high conversion.

4. Conclusions

The third-order nonlinear optical properties of AZO thin films was investigated using z-scan technique with CW He–Ne laser at 633 nm wavelength. They have established that for 1% AZO film, the optical clamping takes place. Whereas for the 3% and 5% AZO films, there is no clamping taking place. In the present case RSA is the leading process for the observed nonlinear absorption. For 1% AZO film, the optical clamping takes place. The films were characterized with a negative nonlinear refractive index. AZO films displayed both SA and RSA absorption behavior. The films exhibited a good optical limiting under the experimental wavelength. The presented results confirms the possibility to use the films as optical limiters and tripled frequency modulators.

Acknowledgements

The authors S. Pramodini and Poornesh P. wish to thank DAE-BRNS bearing sanction no. 2010/20/34/7/BRNS/2263 for funding this research work. For A.H. Reshak his work was supported from the project CENAKVA (No. CZ.1.05/2.1.00/01.0024), and School of Material Engineering, Malaysia University of Perlis, P.O Box 77, d/ a Pejabat Pos Besar, 01007 Kangar, Perlis, Malaysia.

References

- [1] C. Torres-Torres, J.H. Castro-Chacón, L. Castañeda, R. Rangel Rojo, R. Torres-Martínez, L. Tamayo-Rivera, A.V. Khomenko, *Opt. Express* 19 (2011) 16346–16355.
- [2] Vinay Kumari, Vinod Kumar, B.P. Malik, R.M. Mehra, Devendra Mohan, *Opt. Commun.* 285 (2012) 2182.
- [3] Seoung-hwan Park, Doyeol Ahn, *Opt. Quant. Electron.* 38 (2006) 935.
- [4] J. Ebothe, I.V. Kityk, S. Benet, B. Claudet, K.J. Plucinski, K. Ozga, *Opt. Commun.* 268 (2006) 269–272.
- [5] T.M. Williams, D. Hunter, A.K. Pradhan, I.V. Kityk, *Appl. Phys. Lett.* 89 (2006) 043116.
- [6] I.V. Kityk, A. Migalska-Zalas, J. Ebothe, A. Elchichou, M. Addou, A. Bougrine, A.Ka. Chouane, *Cryst. Res. Technol.* 37 (4) (2002) 340–352.
- [7] R. Hansson, P.C. Hayes, E. Jak, *Meta Mater. Trans.* 35B (2004) 633–642.
- [8] T. Yamashita, R. Hansson, P.C.J. Hayes, *Mater. Sci.* 41 (2006) 5559–5568.
- [9] A.O. Fedorchuk, O.V. Parasyuk, I.V. Kityk, *Mater. Chem. Phys.* 139 (2013) 92–99.
- [10] R. Khenata, M. Sahnoun, H. Baltache, M. Rérat, A.H. Reshak, Y. Al Douri, B. Bouhafs, *Phys. Lett. A* 344 (2005) 271–279.
- [11] M. Sheik-Bahae, A.A. Said, E.W. Van Stryland, *Opt. Lett.* 14 (1989) 955–957.
- [12] M. Sheik-Bahae, A.A. Said, T.H. Wei, D.J. Hagan, E.W. Van Stryland, *IEEE J. Quantum Elect.* 26 (1990) 760–769.
- [13] A. Douayar, M. Abd-Lefdil, K. Nouneh, P. Prieto, R. Diaz, A.O. Fedorchuk, I.V. Kityk, *Appl. Phys. B: Opt. Lasers* 110 (2013) 419–423.
- [14] S.S. Shinde, P.S. Shinde, S.M. Pawar, A.V. Moholkar, C.H. Bhosale, K.Y. Rajpure, Physical properties of transparent and conducting sprayed fluorine doped zinc oxide thin films, *Solid State Sci.* 10 (2008) 1209.
- [15] P. Scherrer, *Göttinger Nachrichten* 2 (1918) 98.
- [16] H.I. Elim, J. Yang, J.-Y. Lee, *Appl. Phys. Lett.* 88 (2006) 083107.
- [17] C. Zheng, X.Y. Ye, S.G. Cai, M.J. Wang, X.Q. Xiao, *Appl. Phys. B* 101 (2010) 835–840.
- [18] G. Fan, S. Qu, Q. Wang, C. Zhao, L. Zhang, Z. Li, *J. Appl. Phys.* 109 (2011) 023102.
- [19] P.P. Kiran, N.K.M.N. Srinivas, D.R. Reddy, B.G. Maiya, A. Dharmadhikari, A.S. Sandhu, G.R. Kumar, D.N. Rao, *Opt. Commun.* 202 (2002) 347–352.
- [20] M.G. Vivas, E.G.R. Fernandes, L. R-M Maria, C.R. Mandonca, *Chem. Phys. Lett.* 531 (2012) 173–176.
- [21] S.V. Rao, N. Ventatram, L. Giribabu, D.N. Rao, *J. Appl. Phys.* 105 (2009) 053109.
- [22] P.G.L. Frobel, S.R. Suresh, S. Mayadevi, S. Sreeja, C. Mukherjee, C.I. Muneera, *Mater. Chem. Phys.* 129 (2011) 981–989.
- [23] K.K. Nagaraja, S. Pramodini, H.S. Nagaraja, P. Poornesh, *J. Phys. D Appl. Phys.* 46 (2013) 055106.
- [24] K.K. Nagaraja, S. Pramodini, A. Santhoshkumar, H.S. Nagaraja, P. Poornesh, D. Kekuda, *Opt. Mater.* 35 (2013) 431–439.
- [25] Zouhair Sofiani, Bouchta Sahraoui, Mohammed Addou, Rahma Adhiri, Mehdi Alaoui Lamrani, Leila Dghoughi, Nabil Fellahi, Beata Derkowska, Waclaw Bala, *J. Appl. Phys.* 101 (2007) 063104.